# Study and experimental test of combined harvesting technologies to increase the efficiency of solar energy devices

MASSIMO VISCARDI[1], ROMEO DI LEO[1]

*Abstract:* **-** The present work focuses its attention about the need of implementation of an energy recovery system for a renewable energy device as photovoltaic cells. In a specific way the present paper is addressed to the evaluation of a potential use of Peltier cells to recover waste heat of PV, using the Seedback effect, and the opportunity to recovery the vibrational energy of the PV cell surface when it is subject to the effect of rain drops. An overview of Peltier cells, mainly focused on their functionality, properties and possible applications, is initially presented. The results of an extensive experimental test campaign is then presented; these tests have mainly been dedicated to the  evaluation of Peltier cells properties in the electrical conversion of  heating energy produced and/or not dissipated during the photovoltaic phenomena in siliceous PV cells. The second part of the  work is focuses on a first study for a piezoelectric harvesting system, finalized to obtain electrical energy from the kinetic energy of rainy precipitation;  a renewable energy source not really considered until now. After a state of art of the harvesting systems from environmental energy, linked to vibrations, using piezoelectric structures, and of piezoelectric harvesting systems functioning with rain, authors propose an analysis of the fundamental features of rainy precipitations for the definition of the harvesting system.
An electro-mechanical model for the simulation of performance of the unit for the energetic conversion, composed by three blocks, is proposed. The model is used for a simulation campaign to perform the final choice of the more suitable piezoelectric unit, available on the market, which will be adopted for the realization of the "Piezo Roof Harvesting System".

*Keywords*— Peltier Cell, Photovoltaic Cell, Seedback Effect, Renewable Energy, Energy harvesting, rain, piezoelectric material, mechanical vibration

## I. INTRODUCTION

All scientific community agrees about the idea that conventional sources of energy will finish a day. It is no easy to foresee this day and besides it is a strong challenge to find new energy sources able to override the conventional ones.

In this scenario there is an increasing interest for renewable energy sources as wind and solar energy, which are candidates as future potential contribute for the reduction of consumptions of conventional energy sources or for the complete substitution of them [2].

Solar energy is one of the most widely adopted renewable energy sources, which can be implemented in various applications. For example thermal management using thermal collectors or electricity generation through special optical solar cells as Photovoltaic cells (PV).

PV cells are semiconductor systems, which convert the solar energy in electrical energy.

High capital cost and low conversion efficiency are known as the two main obstacles to globalize the use of solar power and particularly of photovoltaic panels. For this reason the international scientific community is performing any effort to improve the efficiency of conversion of these systems and to increase the final output power obtained.

The efficiency rate of the system depends on the type of semiconductor material, used for the production of the solar cell. At the present in function of the used semiconductor material, the theoretical efficiency varies from 7 and 40% under optimal operating conditions [4].

Besides the semiconductor material, adopted for the construction of the PV cells, many other issues are able to influence the performance of these elements. For example, elevated temperature and dust accumulation are fundamental problems in any application but above all in desert regions with a very hot climate.

The present work focuses its attention on the opportunity of energy harvesting, by the conversion of extra heating energy, into electrical energy, by the use of specific Pelteir devices.

Another strong variable of PV installation is the equivalent light that cen be converted during the year, Cloudy or rainy days are generally identified as energy loosing period, that can strongly effect  the overall performance of the PV system and the relative financial revenue.

Rain falls from the clouds' level, gaining a constant limit velocity of fall when gravity force is equilibrated by the sum of the resistant force, generated from viscous friction, and by the Archimedes pushing force. In this manner raindrops have a kinetic energy. It could be an interesting opportunity,  to convert this kinetic energy in the electric one for harvesting energy from the

---
[1]Department  of Industrial Engineering, University of Naples "Federico II" Via Claudio, 21 – 80125 Naples    ITALY, massimo.viscardi@unina.it

environment, by the use of electro-mechanical devices as those based upon the use of piezoelectric materials.

The use of the environmental energy source of rain pursues a potential advantage as a green production of energy from a new, not conventional, energy source of renewable type.

In a particular manner flexible piezoelectric materials are interesting for power harvesting because they are able to withstand great strains. Larger strains give a major quantity of mechanical energy for the conversion in electrical energy.

In literature a lot of research works about the conversion of environmental energy, linked to vibrations, using piezoelectric, are present.

A fundamental point to gain a better conversion of mechanical energy in the electric one is the choice of the type of piezoelectric material.

Lee, He, Wu and Shih [16] affirm that although piezoceramic materials PZT are widely used in power harvesting field, they present some problematic aspects. In fact PZT materials are very brittle and this property carries strong limitations in the strain which they can sustain without damages. In a particular way PZT are sensitive to the propagation of the fatigue under a cycle of load, characterized by an high frequency.

To override these limitations of PZT piezoelectric material a new class of more flexible piezoelectric material was developed.

Poly-vinylidene-fluoride PVDF is a polymeric piezoelectric material with a great flexibility in comparison to PZT [16].

About the topic of a piezoelectric harvesting system for the conversion of environmental energy, linked to vibrations, there are many research works in literature.

Lee, Joo, Han, Lee and Koh test a PVDF film coated with poly/poly electrodes. PVDF film works from 10Hz to 1MHz without the presence of electrode damage and it obtain an increasing capacity to harvest power during its lifespan [17].

Mohammadi, Khan and Cass study the power generation ability of piezoelectric lead zirconate titanate fibres composites [18].

They highlight that thicker fibrous plates present larger displacements of fibres and samples with smaller diameter of fibres have the highest $d_{33}$ piezoelectric coefficient and lowest dielectric constant, which are both contributes for a more power conversion and consequently for a more efficient harvesting systems [18].

Sodano, Lloyd, Park and Inman in their works perform a compare on the efficiency of three different types of piezoelectric materials [19,20,21]. Classical PZT, macro-fibre composite MFC and a quick pack actuator are considered. Each type of material is excited at resonance, subjected to a 0-500Hz chirp and then each material is subjected to random vibrations. They find that efficiency of PZT is better than other two systems in all conditions, resonance, chirp and random vibrations. Guigon, Chaillout, Jager and Despesse propose a

theoretical study on a possible harvesting raindrop energy system based on a polymeric piezoelectric bands with a length of 100 mm and a width of 3 mm, supported on both the ends [35].

Guigon, Chaillout, Jager and Despesse in another paper complete the study, presenting an experimental work on the piezoelectric system of energy conversion from rain [36].

Biswas, Islam, Sarkar, Desa, Khan and Huq analyze the solution already proposed by the work of Guigon, Chaillout, Jager and Despesse, evaluating the application of this system in the Bangladesh region where the monsoon produces massive rainfall from June to September [37].

The present work focuses its attention on the proposal of the idea of a "Piezoelectric PV modules" as a new energy harvesting system, based on raindrops.

The paper presents a preliminary theoretical and simulative study for the system. The final aim is the conversion of the mechanical kinetic energy of a meteoric precipitation as the rain in electrical energy.

## II. DISSIPATED HEAT OF PV CELLS AND COOLING SYSTEMS

The photovoltaic cell can absorb about 80% of the solar incident energy but only a portion is converted in electrical energy. The residual part will be dissipated as heat, which will carry to an increase in the temperature of the photovoltaic module.

This is due the fact that PV cells convert a certain wavelength of the incoming irradiation (visible spectrum plus some part of the infrared spectrum), that contributes to the direct conversion of light into electricity, while the rest is dissipated as heat [5].

This dissipated heat and the increasing temperature not only have an influence on the efficiency but also on the technical life-time of the cell. Figure 1 shows the influence on the output power of a single-crystalline silicon PV cells for different operating temperatures.

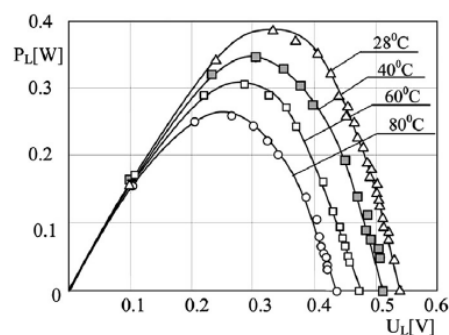Figure 2 illustrates the temperature dependence of the maximum output power [7, 8].



Figure 1: Output power of a single-crystalline silicon PV cells for different operating temperatures.

The function of the efficiency and lifetime of photovoltaic cells with temperature is a potential problem of every application, especially in very hot climate.
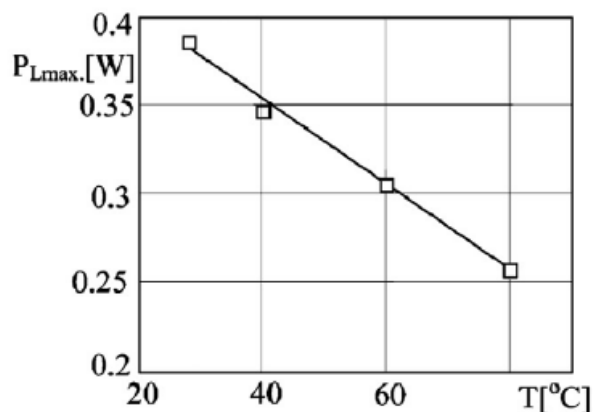


Figure 2: Temperature dependence of the maximum output power for a single-crystalline silicon PV cells.

This great amount of dissipated energy can be converted in electrical energy to improve the total amount electrical energy produced by PV panels and to decrease the temperature of PV modules. In this way, the aim is to increase the production of electrical energy and to prevent excessive cell heating and the consequence of deteriorated performance and lifetime.

Looking at the cooling aspect, there are many possible passive cooling systems as for example the application of bodies constructed with high conductivity materials (for example aluminum, cooper,….) or the application of fins or protruding surfaces to enhance the heat exchange with environment.

Other passive cooling systems are based on the implementation of phase change materials, circuits for the natural circulation or heat pipes.

An example of this typology is a photovoltaic panel for the roof of an house with heat-sinks, installed on the back sheet of the panel. For this system the heat is dissipated in the environment by surfaces of heat-sinks through natural air convection and radiation. Both mechanisms present a low order of magnitude for this reason an active system is required particularly in applications as installations in hot climate places.

The present work proposes to analyze a modified version of passive cooling system based on liquid heat exchanger that use a Peltier element, placed at the interface od PV cell and heat exchanger to produce an extra amount of energy .

In the developments of the present activity the commercial Peltier cells have so been used in an inverse way, utilizing Seedback effect, to produce an electric energy from the thermal gradient on its two faces, produced by the heat dissipated by the PV cell. In this situation the system will be classified as an hybrid photovoltaic-thermal system (PVT) because heat, that is generated by electrical production of PV cells, isn't simply dissipated in the environment but it is used by the system.

In this way waste heat is used to produce an adding share of electricity.

### III. SEEDBACK EFFECT AND PELTIER CELLS

Peltier cells are thermoelectric modules, which present the ability of a direct conversion of thermal energy into electrical one. This is possible thanks to the Seedback effect, discovered by the physicist Thomas Johann Seebeck in 1821. It is a phenomenon in which a temperature difference between two dissimilar electrical conductors or semiconductors produces a voltage difference between the two substances.

The voltages produced are generally small, usually few microvolts per kelvin of temperature difference at the junction. If the temperature difference is large enough, some Seebeck-effect elements can produce few millivolts but numerous elements can be connected in series to increase the output voltage or in parallel to increase the maximum deliverable current.

The Seebeck effect is responsible for the behavior of thermocouples, which are used to measure temperature differences or to actuate electronic switches that can turn large systems on and off status.

The Seebeck effect is a reversible phenomenon; so if it is given an electric current to the structure, which is composed by a joint between two different metals, it is possible to observe that a temperature difference occurs between two different connected metals. This reverse phenomenon is called Peltier effect, in homage to Jean Charles Peltier, who discovered it in 1834.

It's been demonstrated that the Peltier effect occurs not only for the joints between metals but also for those made with semiconductor elements, both natural (silicon, germanium) or artificial.

A common element, which is the basis of a commercial Peltier device, is formed by two dissimilar semiconductor p- and n-.type junctions. These are connected electrically in series and thermally in parallel [12].

Usually to improve the cooling power of cells available on market the common choice is a connection serial-parallel: there are strips made up of individual cells P / N / P (or P / N / N), connected in cascade, in which the area P of the former is electrically connected to the N of the next, and the heads of the individual strips are connected together in parallel.

To hold together the various parts there is a wafer structure which is made by placing side by side all the metal plates that connect the semiconductor with a plate of alumina; they are locked to each other with adhesives designed to withstand temperatures of several tens of degrees Celsius without deformation or softening, such as epoxy resin. Connections in series-parallel of industrial Peltier cells permit the construction of devices operating

at differences of potential from 5 to 20 volts, which can be easily obtained by energy suppliers [13].

Peltier modules possess salient features of being compact, lightweight, noiseless in operation, highly reliable, maintenance free and no moving or complex parts [14, 15].
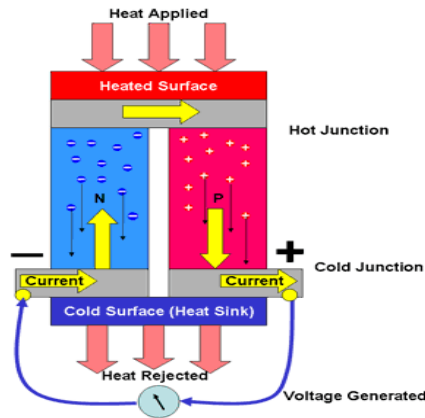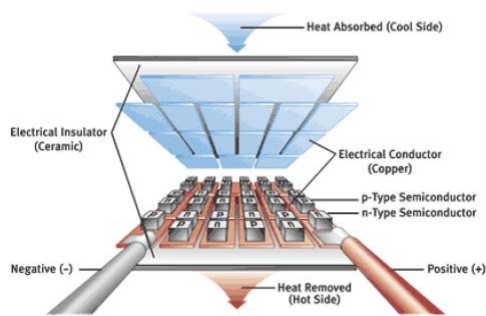


Figure 3: Semiconductor Seedback Effect.



Figure 4: Basic structure of a Peltier cell.

Applying a difference of electrical potential to the cell, which allows a passage of a given current through it, an area cools while the other gives off heat.

In all the application one of the most important parameters to be monitored is the thermal rise that is the temperature difference reached between the hot side and cold side. This temperature difference is specified by the constructor and depends on the current consumption and could be theoretically unlimited: in reality the semiconductor's thicknesses are very thin and so the heat also diffuses to the cold side. For this reason it is necessary to use a system of heat dissipation to achieve the desired amount of cold and to maintain the temperature below a certain level, thus avoiding damage to the device.

Heat sink is addressed to facilitate the passage of heat from the hot side to the external environment, besides it is useful to isolate as much as possible the environment that faces the cold side from that in which the heat sink radiates heat.

Besides in some applications, characterized by the cooling of elements with very small extension, as for example the cooling of an electronic CPU, can be used a coldplate too.

A coldplate is a small thickness of metal, which is interposed between two surfaces of different sizes to optimize the transfer of heat. In fact without the use of a coldplate, a large part of the radiant element (heat sink, the water block or Peltier element) would remain idle as not in contact with the hot part to be cooled.

After an overview on the Peltier cells, on their functionality, properties and possible applications, it is necessary to summarize also their limits, which penalize the use.

The efficiency of the Peltier cell is quite low because the electric energy input is much greater than the thermal energy taken from the cold side and in the reverse use (Seeback effect) only a small fraction of the thermal energy that passes into the cell is effectively converted into electrical energy.

The efficiency $\eta$ is defined as the ratio between the cooling power Pf and the power PD ($I_{max}*V_{max}$) for feeding the cell and is about equal to 0,6.

This feature limits the use of the Peltier cell to applications whose power is much reduced.

Besides as already said in the previous lines, since the cell is crossed by a flow of heat between the two sides, to maximize the difference in temperature compared to the environment of the cold side and to prevent the hot side reaches temperatures harmful to the cell itself, it is necessary to remove the heat generated by heat sinks, radiators or heat pipes. These lasts typically have dimensions and weights over several orders of magnitude compared to the cells themselves. This implies that the size of a thermal system based on Peltier cells depends mainly by the cooling system of the same [14]

The next section presents an experimental analysis of a Peltier cell, which will be used in the subsequent step to improve the amount of energy obtained, generating electrical energy thanks to the use using the heat dissipated by PV module for the Seedback effect (hybrid photovoltaic-thermal system).

## IV. EXPERIMENTAL ANALYSIS

The first experiment campaign [50] has been conducted to evaluate the improvement of power, obtained by PV cell, through the implementation of the Peltier cell, used in a passive way to convert the dissipated thermal energy in electrical one. For this reason it has been prepared the set-up, depicted in figure 5-6 and described in the subsequent lines.
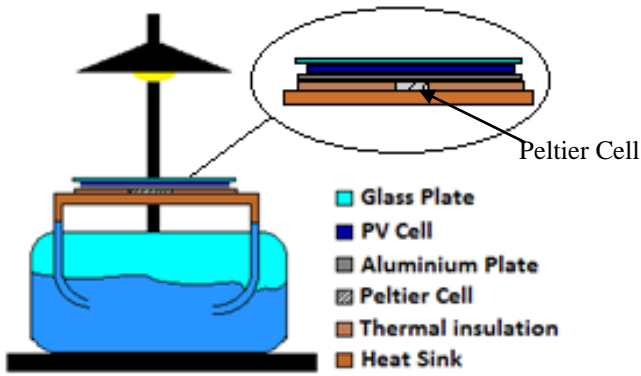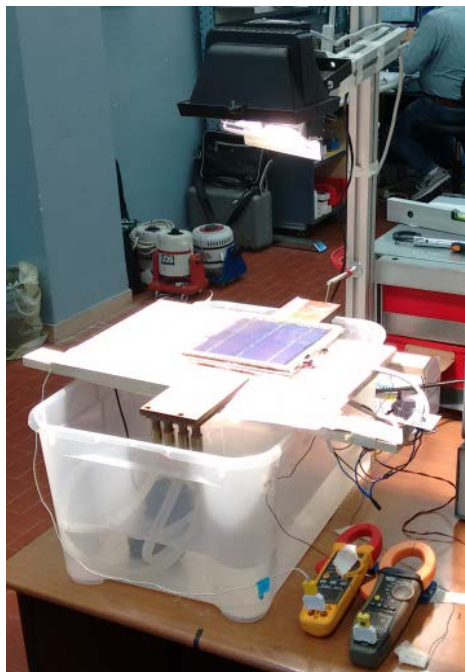
Figure 5: Schematic representation of set up.



Figure 6: Physical realization of Set-up.

The experiments have been conducted using a single photovoltaic cell (Table 1), carefully, covered by a glass plate.

The Photovoltaic cell has been laid on an aluminium plate by means of conductive paste so as to create an homogeneous and improved thermal contact between the two surfaces.

Table 1: Features of PV cell

| Type | Polycrystalline cell |
|------|----------------------|
| Size | 156mm x 156 mm |
| Thickness | 190 $\mu$m |
| Front ( - ) | silver bars for bus (1,6 mm) with anti-reflective coating in blue |
| Rear ( + ) | Bearing sealing off 3mm (Ag), rear surface (Al) |

Because the Peltier cell (Table 2) covers a smaller surface than the photovoltaic cell, it has inserted an insulating sheet of cork, which surrounds the Peltier cell.

Table 2: Features of Peltier cell

| Type | TEC1-12715 |
|------|------------|
| Size | 40mm x 40 mm |
| Thickness | 4 mm |
| Maximum power | 231W (15,4V x 15A) |
| $\Delta T_{max}$ | 70° |
| R($\Omega$) | 1,8 – 2,5 |
| Weigh | 25 gr. |

The Peltier Cell is in direct contact with the aluminium plate through its upper surface (there is only specifically inserted a thin film of conductive paste) and in direct contact with the heat exchanger through its upper surface (there is only specifically inserted a thin film of conductive paste). The heat exchanger is connected through pipes to a reservoir of water at ambient temperature.

To monitor changes in temperatures on the two faces of the Peltier cell and on the upper surface of the PV module, it has been decided to use three thermocouples. The first one is appropriately applied on the upper surface of PV, the others, everyone on a face of the thermoelectric device.

The lighting conditions has been simulated (during this preliminary test campaign) using a 220 V lamp placed at different heights to guarantee laboratory controlled light conditions .

PV module and Peltier cell are electrically linked to a variable electronic load MWL, which allows the adjustment of the level of absorbed current in a range of 0-20 A, by means of a multi-turn potentiometer, that operates at voltages between 0 and 20 V. This instrument was used to detect, to the variation of the electrical load, the characteristic curve V-I or V-R and, therefore, the power supplied by the PV cell and the Peltier cell under different conditions of load.

In this first type of experiment the Peltier cell is used in a passive way. The temperature difference, which is created between the faces of the Peltier cell, due to the heating of the photovoltaic cell and the cooling imparted by the heat exchanger, is used to produce additional energy which is added to that produced by the photovoltaic cell. The experiments have been performed at different heights of the lamp in order to simulate different conditions of light and more in particular different conditions of temperature. The aim of this study is to understand how much additional energy would be produced.

The typical test has performed following the scheme below:

1. Choose the height of the lamp.
2. Turn on or off the heat exchanger pump.
3. Measure the surface temperature of the PV module through the thermocouple.
4. Turn on the lamp.
5. Acquire values for voltage and current through Megaris tester for different applied

electrical loads to obtain the characteristic curve of the module (figure 9).

6. Repeat the previous point for different superficial temperatures of the PV module until the stationary condition is gained.

7. Acquire temperatures of upper and lower faces of Peltier, using thermocouples and its characteristic curve (figure 10), using the Megaris tester.

8. Repeat the previous point for different superficial temperatures of the surfaces of Peltier cell until the stationary thermal condition is gained.

Evaluating the test data performed at different height and temperatures, it's possible to compare, at first, the behavior of the efficiency of the PV cell when the temperature of upper surface of PV panel increases.

Figure 7: P-R curve of PV cell for the Test at height of lamp = 10 cm and the pump of heat exchanger off.
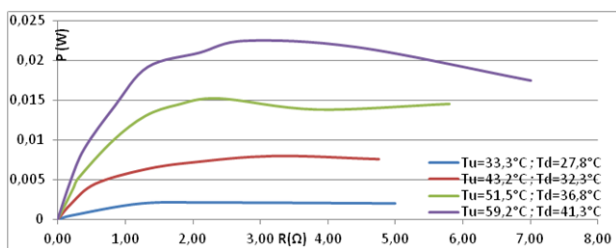


Figure 3: P-R curve of Peltier cell for the Test at height of lamp = 10 cm and the pump of heat exchanger off.

From figure 9 and other graphs about P-R curves of PV cell, referred to different heights of the lamp, it is visible that the maximum power decreases with the increment of the temperature.

Inside each test at a fixed height the luminosity is constant and then the decrease of the maximum power leads to a decrease of the efficiency of the PV cell. The decrement of maximum power in the range of temperature 39-67 °C is approximately 20% equivalent to 7,2% each 10°C. These considerations are supported by table 3:

Table 3: Experimental data.

| H (cm) | Heat Exchanger | | ΔT (°C) | decrease of the maximum power (%) | decrease of the max power each 10°C (%) |
|---|---|---|---|---|---|
| | ON | OFF | | | |
| 45 | | X | 12,5 | 5 | 4 |
| 45 | X | | 9 | 9,1 | 10 |
| 30 | | X | 16,5 | 12 | 7,3 |
| 20 | | X | 28,3 | 19 | 6,7 |
| 20 | X | | 22,7 | 16 | 7 |
| 10 | | X | 46 | 40 | 8,7 |
| 10 | X | | 43,9 | 30 | 6,8 |

where:

H = is the height of the lamp (distance from the lamp and the glass sheet);

ΔT= difference between the maximum temperature of upper face of PV (stationary condition) and its initial temperature in the test.

Figure 11 shows in a clear way (after 36 C°) that at the same upper superficial temperature of the PV module, its performance is the same for tests with heat exchanger pump on and off (respectively named "with" and "without" exchanger). Clearly the maximum temperature in stationary condition will be higher for the pump of heat exchanger "off" than the case "on" as it also evident by values of ΔT, reported in table 3.
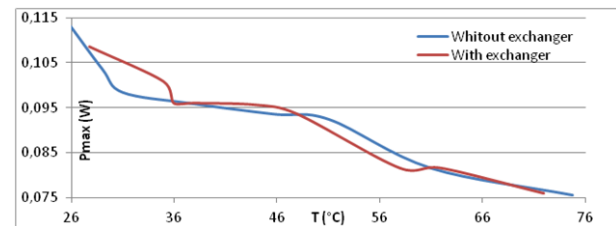


Figure 94: Maximum power of PV cell for different temperatures of its upper surface in cases of pump heat exchanger "on" and "off".

The behavior of the Peltier cell with increasing temperature of upper PV surface is different from that seen for the PV cell. In fact, the maximum power increases with the increment of the temperature (figure 10).

Figure 10: Maximum Power given by Peltier cell versus Superficial Temperature of PV Module

For the Peltier cell the maximum value of the power, obtainable at a temperature of 84 °C, is 89% greater than the value, initially measured at the temperature of 45 °C, corresponding to an increase of 23% every 10 °C. The limit of energy production of the Peltier cell is due to the reduced $\Delta T_{Peltier}$ between its upper and down surfaces as shown by figure 11.
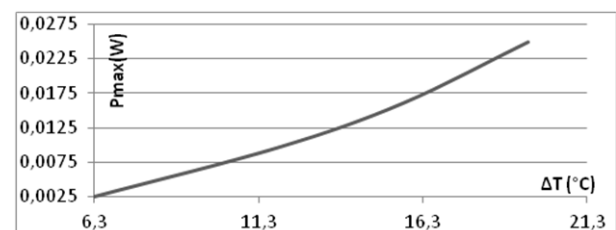


Figure 51: Maximum Power given by Peltier cell versus reduced $\Delta T_{Peltier}$ between its upper and down surfaces.

To increase the electrical power converted by Peltier it is necessary an higher $\Delta T_{Peltier}$. This can be gained by a better system of heat exchanger with the environment and a better isolation system between the back face of the PV panel and the lower face of Peltier. In support of this,

figure 12 shows the difference between the output powers from the Peltier cell in the presence and in the absence of the heat exchanger at the same superficial temperatures of PV module (T=75°C).
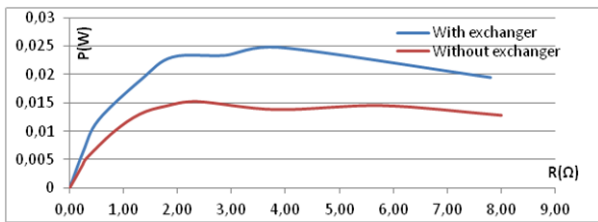


Figure 62: output powers from the Peltier cell for the same superficial temperature with heat exchanger "on" and "off".

During the test, under the described conditions, the maximum $\Delta T_{Peltier,}$ obtained in the Peltier cell, is equal to 23 °C with a power output of 25 mW, corresponding to the 15% of the maximum power produced by the PV module alone in the same operative conditions. The percentage increase of power produced by the system, composed with PV and Peltier Cell together is about 22%.

## V. FEATURES OF RAINY PRECIPITATIONS INTERESTING FOR THE ENERGY HARVESTING SYSTEM

The final aim of this part of the research is the creation of a new PV device, able to the conversion of the mechanical kinetic energy of rain in electrical energy.

As previously described, the presence of a piezoelectric material into the solar cell stratigraphy may be proposed as possible solution.

Under this hypothesis, two parameters of rainfall are fundamental: the mass of water and the final limit velocity of fall.

Clearly we are not interested simply to the total mass of water of a rainfall (measured in mm of water/$m^2$) but it is also important to know each share of this mass which falls with a given final limit velocity.

The final limit velocity is related to the diameter of raindrop.

By this preliminary considerations, the fundamental parameters of raindrop for the research project are:
1. the dimension of raindrop (expressed by the value of its diameter)
2. the limit velocity of the drop.

For the first point it's a focal point to define a distribution law between dimension of raindrops and the nature of rainfall. For this reason, in previous work [50] authors conducted a revision of the state of arte in the scientific literature available.

Considering the results of many studies from Marshall, Langille and Palmer [38], in the proximity of the ground the distribution of the medium dimension of raindrops can be presented by a simple equation :

$$N = (N_0 e^{-\Lambda D})*\delta D \qquad (1)$$

where:
- N is the number of drops with diameter inside the interval [D, D + δD] in a unitary volume
- D is the diameter of the drop
- $N_0$ is an asymptotic value for diameter D which tends to 0.

This parameter is experimentally estimated by authors and it is evaluated equal to 0.08 $cm^{-4}$.
- Λ consider the relation with the intensity R (mm/hr.) of the rain

$\Lambda=41R^{-0.21}cm^{-1}$

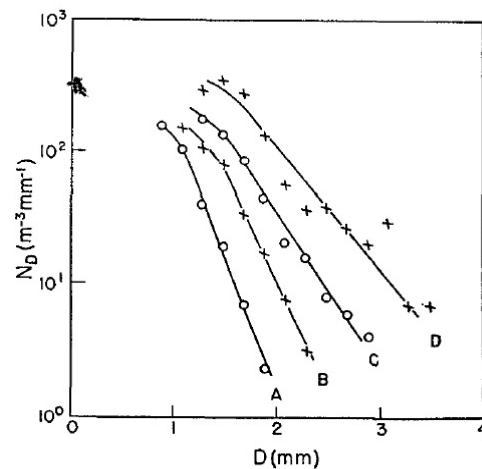This equation is an evolution of the model previously proposed by Laws and Parsons [40].



Figure 13: Curves of Law and Parson in a matching with experimental data

Ryde, develops the model of Marshall and Palmer, introducing the limit velocity of raindrops. He obtains curves of distribution which link the contribution to the mass of water, generated by drops of a defined diameter. These curves are parameterized in function of the intensity of rainfall (mm/hr.) and they present a "bell shape" (14) [41].

The maximum of these curves are approximately distributed on an hyperbolic curve.
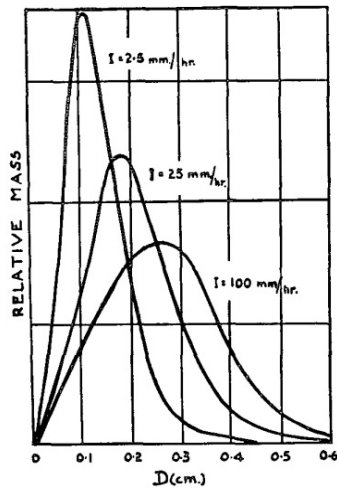
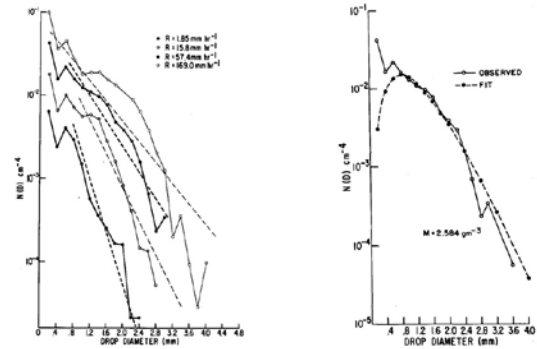Figure 14: Ryde's curves about the distribution of raindrops



Figure 15: On the left side a comparison between experimental data and Marshall and Palmer curves for different level of rain rate. On the right side a comparison between experimental data and Marshall and Willis curve.

Best presents a summary and a comparison about all works on the topic and results obtained [42].

After the study of Marshall and Palmer other researches have been conducted to improve the method.

Sekhon and Srivastava in 1971 conduct an analysis based on a great number of experimental observations, performed with a Doppler radar. For the curves of Marshall and Palmer they identify a new value of intercept with axis D=0 and this value result increasing with the parameter R [29].

Willis and Atmos in 1984 [44] analyse more than one hundred sets of experimental data, obtained by the methodology of the optical spectroscopy. They normalize dimensional distributions and he finds that their trend deviate from the exponential tendency.

The authors consider five types of functions to gain a best fit of data: three exponential functions (as Marshall-Palmer type) and two are a "gamma distribution" type. One of the "gamma distribution" gains the best result about the fitting to the experimental data [44].

In this way he proposes a modification to the widely used Marshall and Palmer method.

In the subsequent curves a comparison is proposed and the behaviour of new model (left side of 15) is better than that of Marshall and Palmer (right side of 15), which present a good matching with observed data for raindrops of medium size but it separates oneself by experimental data for greater or smaller raindrops [44].

In Israel, Feingold and Levin in 1986 carry out two years of measures about the dimensional distribution of raindrops. They confirm that experimental data can be described in a better manner by a not exponential function. They identify a lognormal distribution with a suitable choice of parameters as a better choice than an exponential one (as the equation of Marshall and Palmer). Besides, this description presents the advantage of a physical meaning for their parameters.

In 90's years Sempere Torres, Porra and Creutin demonstrate that it is possible to find an unifying frame for the parameterization of the distribution for the size of raindrops (rainDrop Size Distribution – DSD). This distribution presents all features of a "law of scale". The same authors in 1998 subsequently confirm this idea with a greater number of experimental experiences.

The "law of scale" is clearly function of diameter of raindrop D and of rain rate R.

Following the formalism of "laws of scale" the DSD can be expressed as [47]:

$$N(D,R) = R^{\alpha}g(D/R^{\beta}) \quad (3)$$

Where:
- $N(D,R)$ $(mm^{-1}m^{-3})$ is the rainDrop Size Distribution – DSD, expressed as a function of diameter of the sphere D (mm) equivalent to the raindrop and the rain rate R $(mm\ h^{-1})$
- $\alpha$ e $\beta$ are the "exponents of scale" (not dimensional)
- $g(x)$ is the general distribution of dimensions of raindrops, expressed in function of the scaled diameter of raindrops x= $D/R^{\beta}$

In accordance with the common practice, the rain rate R is generally considered as the reference variable but every macroscopic variable of rain can be used for this aim (for example the factor of radar reflectivity Z).

It is fundamental to highlight that values of α and β and the shape and dimensions of g(x) depend from the choice of the reference variable but they are independent from its value [47].

At the beginning of the present paragraph we highlighted that the second fundamental parameter of raindrop for the research project is its limit velocity.

The first measures about limit velocity were conducted in 70's years when in wind gallery the limit velocity of drops of water was measured in saturated air for different number of Reynolds (0,2- 200). Beard and Pruppacher (1969) measure the dependence of final velocity by Reynolds number of airflow. He highlights

the difference of this final velocity from that of a classical Stokes condition (low Reynolds numbers) [48].

For a rigid sphere in Stokes condition the drag force is:

$$D_s = 6\pi a \eta V_\infty \qquad (4)$$

Where:
- a is the radius of the rigid sphere
- $\eta$ the dynamic viscosity
- $V_\infty$ is the limit velocity.

The value of $D_s$ can be used to obtain a not dimensional graph of real drag force on the raindrop, dividing the measured value of drag force D to the theoretical value $D_s$. The ratio $D/D_s$ is the inverse ratio of $V_s/V$.

Measuring experimentally this last ratio it is possible to evaluate the drag coefficient $C_D$, which is required for a prevision of the limit velocity:

$$V_\infty = \left(\frac{16}{3}\right)\left(\frac{g(\rho_s - \rho_m)}{\eta}\right)\left(\frac{a^2}{C_D R}\right) \qquad (5)$$

with $\rho_s$ and $\rho_m$ respectively the density of the water drop and air (environment in which raindrop fall).

The subsequent image (16) shows the estimation of $C_D$, based on experimental measures in function of Reynolds number in a comparison with the theories of Stokes and Oseen for the velocity of fall.
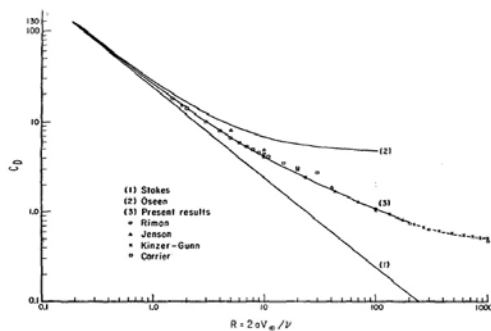


Figure 16: Measured drag coefficient in a comparison with the results of theories of Stokes and Oseen

This measure through the Reynolds number depends by many physical parameters (diameter of the drop, temperature, humidity and atmospheric pressure).

This measure is a useful manner to estimate the limit velocity in fact the subsequent quantity is a function only of environmental parameters and raindrop's diameter:

$$C_D R^2 = \left(\frac{32}{3}\right) a^3 (\rho_s - \rho_m)\left(\frac{\rho_m g}{\eta^2}\right) \qquad (6)$$

Assigned the value of $\rho_s$, $\rho_m$ and dynamic viscosity $\eta$ (function of humidity and temperature) and the raindrop's radius a, it is possible to estimate the Reynols number, inverting the previous expression. In this way using the known value of $C_D$ and R, it is possible to estimate the limit velocity with the expression

$$V_\infty = \frac{R\eta}{2\rho_m a} \qquad (7)$$

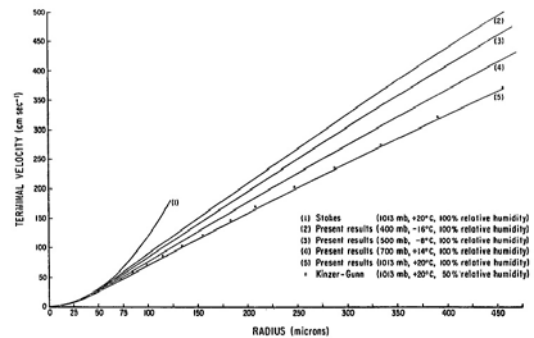Figure 17 reports some estimations, made with this technique [48].



Figure 17: Limit velocity of raindrops calculated with the procedure presented by Beard and Pruppacher

In a rainy phenomena not all drops fall effectively at their limit velocity. Recent use new techniques for the measure of the falling drops, show that some drops have a limit velocity of one order of magnitude greater than the expected limit velocity [49]. These drops, called "Super-terminal", carry to an increase of the real energy available against the expected one. For this reason in the case of an harvesting application these "Super-terminal drops" can be neglected in the energy estimation in a first approximation.

In the present work to estimate the limit velocity of raindrops we use the relation, obtained by Guigon R. in 2006 considers weight "W", viscous friction "R" and Archimedes' push "A" as forces acting on the raindrop [19].

Solving the second equation of dynamic

$$\vec{A} + \vec{W} + \vec{R} = m\vec{a} \qquad (8)$$

it is possible to calculate the velocity of a drop in function of its height of fall.

$$V(H) = \frac{1}{\alpha} * \sqrt{1 - 4 * e^{-H*\alpha*b + \alpha + b*A}} \qquad (9)$$

with:

$$m = \rho_{water} * \frac{\pi D^3}{6}; \qquad m' = \rho_{air} * \frac{\pi D^3}{6};$$

.
k

$$; \qquad \mu = \frac{m - m'}{m}$$

and

$$\alpha = \frac{\ln(1 + \alpha * V_{init})}{1 - \alpha * V_{init}} \quad ;$$

$$b = 2 * \alpha * \mu * g \quad ; \qquad A = \frac{-2\ln(e^{\alpha} + 1)}{b}$$

The third fundamental feature of rainy precipitation, interesting for an energy harvesting system is the annual quantity of water fallen in a region.

Figure 18 shows that the region with the greatest annual rainfall (measured as mm/year for every on a square meter) are located in South America, Africa and South-east of Asia (regions of monsoons) with an annual precipitation of about 3000mm/year.

In a detail about Italy, Alpine arch and Apennines ridge are the zones with the greatest annual rainfall (about 1500 mm/year).
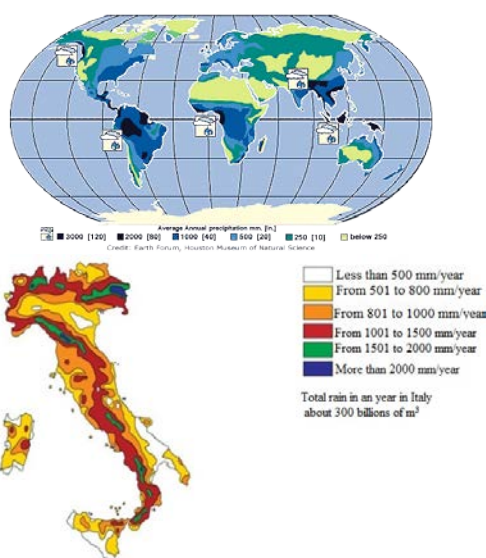


Figure 18: Annual rainfall in the world and in Italy (mm/a)

Clearly the system proposed in the present study presents a more potentiality in the region with high annual rainfall with a consequent higher temporal density of energy.

All considerations about features of rain, interesting to the energy harvesting system, exposed in the rows of this paragraph will be useful not only for the study of the system but also for an analysis about economic, social and environmental impact of the proposed piezoelectric energy harvesting system.

## VI. KEY PATTERNS FOR A PIEZOELECTRIC ENERGY HARVESTING SYSTEM.

Some key patterns for the realization of a piezoelectric energy harvesting system, using rainfall, has been evaluated [--].

Along them, the ideal pattern that contemplate the implementation of a piezoelectric patch, bonded by a glue to a membrane. The membrane (the PV cell) has a fixed constrain on its four edges.
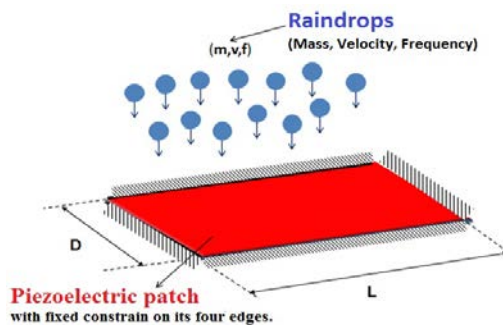


Figure 19: Ideal concept n°1

The membrane subjected to the loads, generated by impacts of raindrops with its surface, generates a deformation of the membrane and consequently of the bonded piezoelectric patch.

This conceptual scheme, does not represent the most effective one [50] , since the strain distribution along the element cannot be maximized because of the element stiffness and the relative boundary conditions, but represent the closest scheme to the real application configuration.

## VII. CHOICE OF PIEZOELECTRIC MATERIAL AND ELECTRO-MECHANICAL MODEL OF SIMULATION

After the choice of a key pattern it is necessary to answer to the question "what is the best material for the final aim"?

A market research, involving the main manufacturers of piezoelectric materials has been performed.

The first one is constituted by a piezoceramic Lead Zirconate Titantate PZT material the second one by a polymeric material PolyVinyliDene Fluoride PVDF.

After the analysis of the technical datasheets of different piezoceramic PZT materials, built by different manufacturers and different PZT patches, PI DuraAct P.876-A11, constituted by Pic255 material, appears as the most convenient one. The piezoelectric material Pic255 is covered on each side by a layer of a polymeric material, named Kapton.

In fact DuraAct P.876-A11 presents the greatest flexibility for bending loads. This advantage of the greatest bending flexibility is joined to the greater value of electromechanical coupling factor of the material PIC252 than PZT materials of others manufacturers.

The electromechanical coupling factor together with variation of deformation influences the quantity of electrical energy, extracted by a piezoelectric in an application of energy harvesting. Inside the DuraAct family P.876-A11 presents the higher capacity (150 ηF) and the smallest bending radius (12 mm).

The same logic process has carried to select the PVDF patch Measurement Specialties LDT1-028K.

The selected PVDF patch presents a greater flexibility than PZT P.876-A11 but a smaller electromechanical

coupling factor. About these two physical aspects the two patches follow the general behavior existing between PZT and PVDF material.

The piezoelectric material PVDF is covered on each side by a layer of a polymeric material, named Kapton.

Table 4: Piezo technical data

| Technical Data | Piezo P-876.A11 |
|---|---|
| Operating Voltage | -20 to +200 V |
| Lateral Contraction, open-loop | 400µm/m 1,6 µm/(H/mV) |
| Holding Force | 90 N |
| Length/Width/Thickness | 61 mm/35 mm/0,4 mm |
| Bending radius | 12 mm |
| Piezo ceramic Type | Pic 252 – Layer Thickness 100 µm |
| Electrical Capacitance | 150 ηF |

Clearly an higher flexibility pushes in the direction of a better energetic conversion and the same is made by an higher electromechanical coupling factor. It is necessary to understand inside the selected PZT and PVDF patch, which presents the best tradeoff and consequently the best performance.

For this reason authors elaborate an electromechanical model to simulate performance of the system about the final energetic conversion for each patch.

The proposed model is composed by three blocks:
- ✓ Mechanical model of piezoelectric patch
- ✓ Mechanical model of the raindrop
- ✓ Model for the prevision of the electrical energy converted

Output data of the blocks 1 and 2 are the input for the third block. In more detail the block n°1 models the mechanical behavior of a piezoelectric patch subjected to the action of the impact with a raindrop. In this part of the model the raindrop's impact is modeled with a time history of force applied in the region of impact between the surface of the patch and the raindrop.

For this aim the F.EM. approach is used through a software LS-DYNA 971 R4. In this software it builds a F.E.M mechanical model of analyzed piezoelectric patch.

PZT P.876-A11 is modeled through 2964 elements of shell type with variable dimensions between 0,5 and 1 mm. Mechanical properties of layers in PIC252 and Kapton materials are adopted in the model, using the formulation of composites in the region of overlapping between Kapton and PIC252.

The scheme, modeled, is a cantilever beam with a constraint of fixed support on the short side and a free span of 41 mm.

PVDF LDT1-028K is modeled through 1488 elements of shell type with variable dimensions between 0,5 and 0,9 mm. Mechanical properties of layers in PVDF and Mylar materials are adopted in the model, using the formulation of composites in the region of overlapping between Mylar and PVDF.
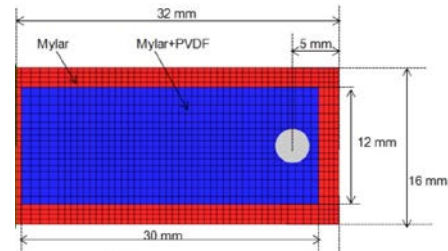


Figure 20: F.E-M. model of Measurement Specialties LDT1-028K

The second block of the electromechanical model simulates the raindrop.

A F.E.M. model of raindrop is created and it is validated through the results of a previous C.F.D. study also performed by authors.

The C.F.D. analysis uses an approach with VOF (Volume of Fluid) methodology to simulate a multiphase problem as the impact of a raindrop against an infinitely rigid surface.

The aim of C.F.D. study is the evaluation of the impact force of a raindrop against an assigned surface. Then it will be used as a comparative term to validate the F.E.M. model which is able to calculate deformations of piezoelectric patches and consequently the electric energy achievable.

In the C.F.D. analysis a 2D and a 3D computational model are built. They are both composed by cells with a dimension of 0,05 mm, considering that the dimension of raindrop falls inside the order of magnitude of some millimeter.

Many simulations have been performed, varying parameters and conditions as the diameter of raindrop, the velocity of impact and the presence or the absence of a water film on the surface.

It is possible to highlight the similarity of results generated by 2D and 3D model. The numerical results present a lower peak of force than experimental one but after the first phase of impact their trend matches the experimental one in a good way. However the numerical results give a longer time with higher forces than the experimental one, for this reason the area under the green rectangle and blue rectangle are similar.

For the present problem the impulse of the force is fundamental aspect for this reason, it's possible to affirm that the numerical model gives a good description of experimental phenomena.
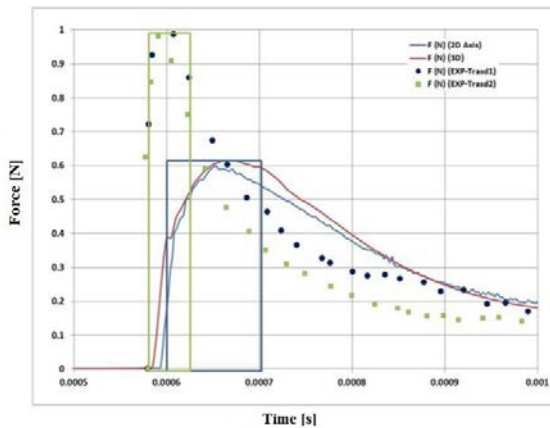
Figure 21: Results of 2D and 3D C.F.D models compared with experimental data in the case of a raindrop with a diameter of 3,3 mm and a limit velocity of 8,32 m/s and in absence of water film on the surface.

The third part of the model is addressed to the estimation of the final electric energy converted by a piezoelectric unit after the impact with the drop, simulated in the F.E.M section of the model.

This last section of the model is based on a numerical model, used by Courbon (1988) and implemented in the present activity in an Excel sheet.

Equations for the calculation are:

$$U_{elec} = \frac{(K^2 * Y * \theta * S^2_{Aver})}{2} \quad (10)$$

with:

K = coefficient of coupling of the piezoelectric material; Y = modulus of Young of the piezoelectric material; $\Theta$ = active volume (is the volume of the piezoelectric material);

$$S_{aver} = \frac{1}{(b-a)} * \int_a^b Sr(x_i, t) dx \quad ;$$

where:

- $Sr(x_i, t)$ is the difference of strain in the same point but in two consecutive instants of time

Then:

-;

- a= initial abscissa (in the longitudinal direction) of the piezoelectric material;
- b= final abscissa (in the longitudinal direction) of the piezoelectric material;
- b-a = free length of the piezoelectric material;

Clearly a e b terms depend from the reference system selected in the simulation.

## VIII. RESULTS OF SIMULATION CAMPAIGN

After the presentation of three blocks, composing the electromechanical model, results of a simulation campaign are reported in the present section.

Simulations are performed for PVDF LDT1-028K and PZT P.876-A11 , but will be reported only for the

PVDF solution, because it has been identified as most suitable piezoelectric device for the application proposed. For the PVDF LDT1-028K the subsequent data are inserted in the electromechanical model:

- $K_{31}$=0,120;      $\Theta$= 1*w*t =10,1*10$^{-9}$m$^3$;   b-a=30mm=0,03 m;
- Y = Young's Modulus = 3 *10$^9$ N/m$^2$;

The simulation case chosen is a raindrop with a diameter of 3,3 mm and a limit velocity of 8,3 m/s, which strikes the piezoelectric surface of PVDF element .

Output of the electromechanical model for the PVDF is reported in the Figure 22 as electric energy converted.

Then from energy converted through a derivative operation in the time, an estimation of power is reported.
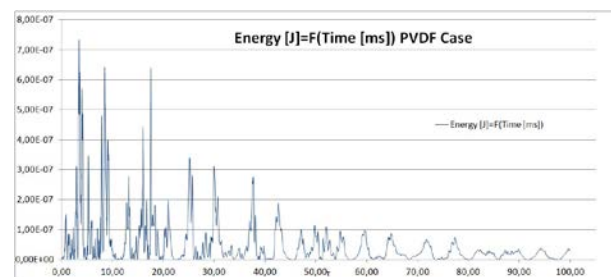


Figure 22: Electrical energy (J) converted by PVDF patch from an impact with a raindrop with a diameter of 3,3 mm and limit velocity of 8,3 m/s vs time (ms)
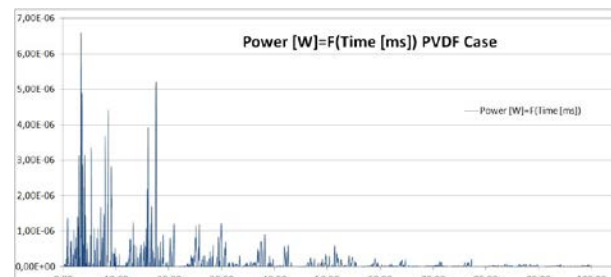


Figure 7: Power (kW) of PVDF vs time (ms)

The maximum value of energy converted by piezoelectric PVDF during its deformation is 0,73 µJ at 3,5 ms after the beginning of the impact. The maximum power is 6,5 mW (Figure 23) for each single PVDF element area.

If a PVDF element covering the whole area of the PV cell is used, an equivalent Power of 122mW is expected.

PVDF LDT1-028K has been selected instead of PZT element, because it presents a lower coupling coefficient and a lower active volume than PZT P.876-A11 (a disadvantage for the final performance of the device for energetic conversion) but higher performances. The explanation is in the very greater elasticity of PVDF material than PZT one. In the present study the exciting force is very low because it is an impact force of a raindrop against a flexible surface. For this reason the more elastic material present a bigger variation of

deformation in the time then the largest conversion of energy.

Besides PVDF LDT1-028K guarantees other two advantages.

The first one is a less surface of the device and consequently a greater energy density.

The second one is a very lower price than PZT device. This is a fundamental topic for a future realization of a "Piezoelectric Solar Cell" .

## IX. CONCLUSIONS

The present  work has been addressed to two focal points: the first concerns the problem of recovering the dissipated heat from the lower face of the PV cell when it is stricken by a light, the second one is the development of  a piezoelectric harvesting system, finalized to the obtaining of electrical energy from the kinetic energy of rainy precipitation, a renewable energy source not really considered until now.

Experimental test based on the use of Peltier cell bonded on the back of a PV cell have been demonstrated that an additional amount of energy may be extracted from the system converting a portion of the thermal energy into electrical one. This amount has been quantified into about the 22 % of the direct photovoltaic energy, and would represent a direct increment of the system efficiency.  At the same time, the presence of a fluid heating exchanger in the system, let the recovery of additional thermal energy for fluid heating; this fluid will be than used in a more conventional way (water heating).

To increment the overall performance of the PV module, intended as the equivalent hours of work per year, a different technology has been imaged to be introduced, to let the PV module work also in rainy days.

After a state of art of the harvesting systems from environmental energy, linked to vibrations, using piezoelectric structures, and of piezoelectric harvesting systems functioning with rain, authors has proposed an analysis of the fundamental features of rainy precipitations for the definition of the harvesting system.

Then, the most suitable  key patterns for the realization of the piezoelectric energy harvesting system have discussed and analysed, presenting their relative advantages and disadvantages. An  electro-mechanical model for the simulation of performance of the unit has been also introduced.

The final choice has fallen on a PVDF material for its greater elasticity; this material cen be easily introduced in the layering of the module or can be glued on the bask sheet of the system.

First computational consideration, let assume that power production by the use of this functionality, does not strongly differ from the solar energy production. This consideration, if confirmed, directly would extend the overall module working hours per year.

*References:*

[1] AA.VV., Energy Outlook 2013 dell'EIA, *EIA Energy Information Administration,* 2013

[2] Di Leo R., Viscardi M., Ferrini G. and. Lecce L, Preliminary Theoretical Study about a "Piezoelectric Shingle" for a Piezoelectric Energy Harvesting System in Presence of Rain*, Mathematical and Computational methods in Electrical Engineering "Proceedings of the 2th International Conference on Power and Energy, System, POES'15, Malta, August 2015.*

[3] Kurtz S., Opportunities and challenges for development of matureconcentrating photovoltaic power industry, *National Renewable Energy Laboratory,* 2011, 5200–43208 (NREL/TP).

[4] Website of European Commision, http://ec.europa.eu/europe2020/europe-2020-in-a-nutshell/targets/index_en.htm

[5] Luque A, Hegedus S., Handbook of photovoltaic science and engineering. 2nd ed., 2011, West Sussex, John Wiley & Sons.

[6] Chatterjee S. ,TamizhMani G., BAPV arrays: side-by-side comparison with and without fan cooling., in IEEE photovoltaic specialists conference (PVSC), 2011, vol 7, pp537–542.

[7] Radziemska E., The effect of temperature on the power drop in crystalline silicon solar cells. *RenewableEnergy*, 2003, 28, pp.1–12.

[8] Makki A., Omer S., Sabir H., Advancements in hybrid photovoltaic systems for enhanced solar cells performance, *Renewable and sustainable energy reviews*, 41, 2005, pp. 658-684.

[9] Teo H. G., Lee P.S., Hawlader M.N.A., An active cooling system for photovoltaic modules, *Applied Energy*, 90, 2012, pp. 309-315.

[10] Royne A., Dey C.J., Mills D.R., Cooling of photovoltaic cells under concentrated illumination:  a critical review. *J. Solar Energy Solar Cell*, 2005, 86, pp. 451–483.

[11] Najafi  H, Woodbury K.A., Optimization of a cooling system based on Peltier effect for photovoltaic cells, *Sol Energy*, 2013, 91, pp.152–60.

[12] Elsheikh H.M., Shnawah D.A., SabriM.F.M., Said S.B.M., Hassan H.M., Bashir A.M.B. et al., A review on thermoelectric renewable energy: principle parameters that affect thei performance, *Renewable Sustainable Energy* Rev. 2014, 30, pp. 337–355.

[13] Omer S.A., Infield D.G.,.Design optimization of thermoelectric devices for solar power generation, *Sol Energy Mater Sol. Cells*, 1998, 53, pp.67–82.

[14] Ahiska R,, Dislitas S., Omer G., A new method and computer-controlled system for measuring the time constant of real thermoelectric modules, Energy Convers Manage, 2012, 53(1), pp.314–321.

[15] Lee BS, He JJ, Wu WJ and Shih WP (2006) MEMS generator of power harvesting by vibrations using piezoelectric cantilever beam with digitize electrode. Proceedings of Smart Structures and Materials Conference. Proc. SPIE 6169 61690B

[16] Lee CS, Joo J, Han S, Lee JH and Koh SK (2005) Poly(vinylidene fluoride) transducers with highly conducting poly(3,4-ethylenedioxythiophene) electrodes. Proceedings of International Conference on Science and Technology of Synthetic Metals vol. 152 pp 49–52

[17] Mohammadi F, Khan A and Cass RB (2003) Power generation from piezoelectric lead zirconate titanate fiber composites. Proceedings of. Materials Research Symposium. p. 736

[18] Sodano HA, Lloyd J and Inman DJ (2004) An experimental comparison between several active composite actuators for power generation. Proceedings of Smart Structures and Materials Conf.; Proc. SPIE 5390 370–8

[19] Sodano HA, Park G and Inman DJ (2004) A review of power harvesting using piezoelectric materials. Shock Vibration Digest 36 pp.197–206

[20] Sodano HA, Park G and Inman DJ (2004) Estimation of electric charge output for piezoelectric energy harvesting. Strain 40 pp. 49–58

[21] Baker J, Roundy S and Wright P (2005) Alternative geometries for increasing power density in vibration energy scavenging for wireless sensor networks. Proceedings of 3rd International

Energy Conversion Engineering Conference (San Francisco, CA, Aug.) pp 959–70

[22] Platt SR, Farritor S and Haider H (2005) On low-frequency electric power generation with PZT ceramics. IEEE/ASME Trans. Mechatronics 10 pp. 240–52

[23] Ng TH and Liao WH (2005) Sensitivity analysis and energy harvesting for a self-powered piezoelectric sensor. Journal of Intelligent Material Systems and Structures 16 785–97

[24] Roundy S (2005) On the effectiveness of vibration-based energy harvesting, Journal of Intelligent. Material Systems and Structures. 16 809–23

[25] Benasciutti D, Brusa E, Moro L and Zelenika S (2008) Optimised piezoelectric energy scavengers for elder care. Proceedings of 10th International EUSPEN Conference, Zurich, 41-45, 2008

[26] Mateu L and Moll F (2005) Optimum piezoelectric bending beam structures for energy harvesting using shoe inserts., Journal of Intelligent Material Systems and Structures 16 835–45

[27] Mossi K, Green C, Ounaies Z and Hughes E (2005), Harvesting energy using a thin unimorph prestressed bender: geometrical effects. Journal of Intelligent Material Systems and Structures 16 249–61

[28] Ericka M, Vasic D, Costa F, Poulin G and Tliba S (2005) Energy harvesting from vibration using a piezoelectric membrane. Journal Physique. Coll. IV 128 187–93

[29] Kim S, Clark WW and Wang QM (2005) Piezoelectric energy harvesting with a clamped circular plate: analysis. Journal of Intelligent Material Systems and Structures 16 847–54

[30] Kim S, Clark WW and Wang QM (2005) Piezoelectric energy harvesting with a clamped circular plate: experimental study. Journal of Intelligent Material Systems and Structures 16 855–63

[31] Han J, Von Jouanne A, Mayaram K and Fiez TS (2004) Novel power conditioning circuits for piezoelectric micro power generators. Proceedings of 19th Annual IEE Applied power electronics conference and exposition pp. 1541-6

[32] Lefeuvre E, Badel A, Richard C, Petit L and Guyomar D (2006) A comparison between several vibration-powered piezoelectric generators for standalone systems. Sensors Actuators A 126 405-16.

[33] Premount A (2006) Mechatronics: Dynamics of electromechanical and piezoelectric systems, Springer Editor

[34] Guigon R, Chaillout JJ, Jager T and Despesse G (2008) Harvesting raindrop energy: theory. Smart Materials and Structures 17

[35] Guigon R, Chaillout JJ, Jager T and Despesse G (2008) Harvesting raindrop energy: experimental study. Smart Materials and Structures 17

[36] Biswas PV, Islam MA, Sarkar MAR, Desa VG, Khan MH and Huq AMA (2009) Harnessing raindrop energy in Bangladesh. Proceeding of the International conference on mechanical engineering, Dhaka, Bangladesh

[37] Marshall JS, Langille RC, and Palmer WK (1947) Measurement of rainfall by radar. Journal of. Meteorology 4, 186–192

[38] Marshall JS and Palmer WMcK (1948) The distribution of raindrops with size. McGill University, Montreal

[39] Laws JO and Parsons DA (1943) The relation of raindrop-size to intensity. Natural Research Council American Geophysical Union Transaction, 24, part II, pp 452-460

[40] Ryde W (1946) The attenuation and radar echoes produced at centimetre wavelenghts by various meteorological phenomena. Journal of, Metereological factors in radio wave propagation, London, The Physical Society, pp 169-188

[41] Best AC and. Roy QJ (1950) The size distribution of raindrops. Meteorological. Society, 76, 16-36, 1950

[42] Sekhon RS, Srivastava RC (1971) Doppler Radar Observations of Drop-Size Distributions in a Thunderstorm. Journal of Atmospheric Sciences, vol. 28, Issue 6, pp.983-994, 1971

[43] Willis PT and Atmos J (1984) Functional fits to some observed drop size distributions and parameterization of rain. Journal of the Atmospheric Sciences, 41, 1648-1661

[44] Feingold G and Levin Z (1986) The lognormal fit to raindrop spectra from frontal convective clouds in Israel. Journal of Applied. Meteorology, Vol. 25, 1346-1363

[45] Sempere Torres D, Porra JM, and Creutin JD (1994) A general formulation for raindrop size distribution. Journal of Applied Meteorology and Climatology vol. 33, pp. 1494-1502, 1994

[46] Sempere Torres D, Porra JM, and Creutin JD (1998) Experimental evidence of a general description of raindrop size distribution properties. Journal of Geophysical Research (D), vol. 103, pp. 1785-1797

[47] Beard KV and Pruppacher HR (1969) A Determination of the Terminal Velocity and Drag of Small Water Drops by Means of a Wind Tunnel., Journal of Atmospheric Sciences, vol. 26, Issue 5, pp.1066-1072

[48] Montero-Martinez G, Kostinski AB, Shaw RA and Garcia-Garcia F (2009) Do all raindrops fall at terminal speed? Geophysical Research Letters, Vol. 36, L11818, Doi:10.1029/2008gl037111

[49] Nearing MA, Bradford JM and Holtz RD (1986) Measurement of force vs time relations for waterdrop impact" Soil Science

[50] Viscardi M. , Di Leo R., (2016) Study and experimental test of Peltier cells for an energy recovery system in a renewable energy device WSEAS TRANSACTIONS on ENVIRONMENT and DEVELOPMENT, Volume 12, 2016 pag 343-352